

# Synaptic Integration in Rat Frontal Cortex Shaped by Network Activity

Jean-François Léger,<sup>2</sup> Edward A. Stern,<sup>3</sup> Ad Aertsen,<sup>1</sup> and Detlef Heck<sup>4</sup>

<sup>1</sup>Neurobiology and Biophysics, Department of Biology III, Albert-Ludwigs-University, Freiburg, Germany; <sup>2</sup>Laboratoire de Neurobiologie Cellulaire et Moléculaire, Centre National de la Recherche Scientifique Unité Mixte de Recherche 8544, Ecole Normale Supérieure, Paris Cedex, France; <sup>3</sup>Department of Neurology, Massachusetts General Hospital, Charlestown, Massachusetts; and <sup>4</sup>Department of Anatomy and Neurobiology, University of Tennessee, Health Science Center, Memphis, Tennessee

Submitted 24 January 2003; accepted in final form 5 August 2004

**Léger, Jean-François, Edward A. Stern, Ad Aertsen, and Detlef Heck.** Synaptic integration in rat frontal cortex shaped by network activity. *J Neurophysiol* 93: 281–293, 2005. First published August 11, 2004; doi:10.1152/jn.00067.2003. Neocortical neurons in vivo are embedded in networks with intensive ongoing activity. How this network activity affects the neurons' integrative properties and what function this may imply at the network level remain largely unknown. Most of our knowledge regarding synaptic communication and integration is based on recordings in vitro, where network activity is strongly diminished or even absent. Here, we present results from two complementary series of experiments based on intracellular in vivo recordings in anesthetized rat frontal cortex. Specifically, we measured 1) the relationship between the excursions of a neuron's membrane potential and the spiking activity in the surrounding network and 2) how the summation of several inputs to a single neuron changes with the different levels of its membrane potential excursions and the associated states of network activity. The combination of these measurements enables us to assess how the level of network activity influences synaptic integration. We present direct evidence that integration of synaptic inputs in frontal cortex is linear, independent of the level of network activity. However, during periods of high network activity, the neurons' response to synaptic input is markedly reduced in both amplitude and duration. This results in a drastic shortening of its window for temporal integration, requiring more precise coordination of presynaptic spike discharges to reliably drive the neuron to spike under conditions of high network activity. We conclude that ongoing activity, as present in the active brain, emphasizes the need for neuronal cooperation at the network level, and cannot be ignored in the exploration of cortical function.

## INTRODUCTION

A single pyramidal cell in the rat neocortex receives synaptic inputs from about 10,000 neurons (Larkman 1991), each of which fires action potentials at an average rate between 1 and 10 per second in vivo (Abeles et al. 1990). As a result, there is a considerable amount of ongoing activity in the network, which is known to influence the response characteristics of individual neurons (Arieli et al. 1996; Azouz and Gray 1999; Tsodyks et al. 1999). How each neuron integrates its synaptic input and what are the time constants involved are crucial for the functioning of the network (Abeles 1982; Diesmann et al. 1999; König et al. 1996). Large integration time windows are usually associated with encoding by spike rates, whereas small integration time windows are associated with encoding by precisely timed spike patterns (Riehle et al. 1997; Steinmetz et al. 2000). The integration properties of cortical neurons have mostly been studied in vitro (Magee 2000; Yuste and Tank 1996). Unlike the intact brain, however, in vitro

preparations show a strongly reduced network activity, or none at all. Several factors tend to indicate that this absence of network activity could introduce an important bias when measuring neuronal integrative properties. For instance, it has been predicted on the basis of theoretical studies (Bernander et al. 1991; Destexhe and Paré, 1999; Rapp et al. 1992) and experimentally observed (Borg-Graham et al. 1998; Paré et al. 1998) that variations of network activity in vivo are associated with changes in input resistance and membrane time constant because of the opening of large numbers of postsynaptic ion channels. Such network activity-dependent modulation of a neuron's membrane properties are likely to affect the summation of inputs taking place in that neuron. Thus neuronal integrative properties in vivo may well deviate from in vitro observations.

To specifically evaluate the influence of ongoing network activity on synaptic integration and to assess its functional consequences, we performed simultaneous extra- and intracellular in vivo recordings in neocortical neurons, under conditions of strong spontaneous modulations of network activity. Specifically, we made use of the fact that pyramidal neurons in the rat neocortex express membrane potential fluctuations where hyperpolarized, quiescent periods alternate with depolarized periods with large voltage fluctuations and spike activity. An example of such membrane potential fluctuations in a frontal cortex neuron is shown in Fig. 1A (*top trace*). The corresponding amplitude probability distribution of the signal is shown on the right, with bars marking the voltage ranges that were later analyzed separately. Such depolarized and hyperpolarized periods were termed "up" and "down" states when first described (Cowan and Wilson 1994; Steriade et al. 1993), and correspond to periods of intensive and sparse network activity, respectively (Amzica and Steriade 1995; Stern et al. 1997; see also Fig. 1A, *bottom traces*). We thus characterized the window for temporal integration at different levels of network activity by measuring the summation of synchronized and nonsynchronized postsynaptic potentials (PSPs) in the associated regimes of membrane potential fluctuations. Preliminary results were presented in abstract form (Heck et al. 2000).

## METHODS

All animal experiments were carried out in accordance with the Freiburg University's and German national guidelines on the use of animals in research.

Two series of experiments were performed. In the first one, simultaneous intra- and extracellular recordings were performed to investigate the relationship between a single neuron's membrane potential and the variations of activity in its surrounding network. In the second series,

Address for reprint requests and other correspondence: D. Heck, University of Tennessee Health Science Center, Dept. of Anatomy and Neurobiology, 855 Monroe Ave., Room 405, Memphis, TN 38163 (E-mail: dheck@utmem.edu).

The costs of publication of this article were defrayed in part by the payment of page charges. The article must therefore be hereby marked "advertisement" in accordance with 18 U.S.C. Section 1734 solely to indicate this fact.

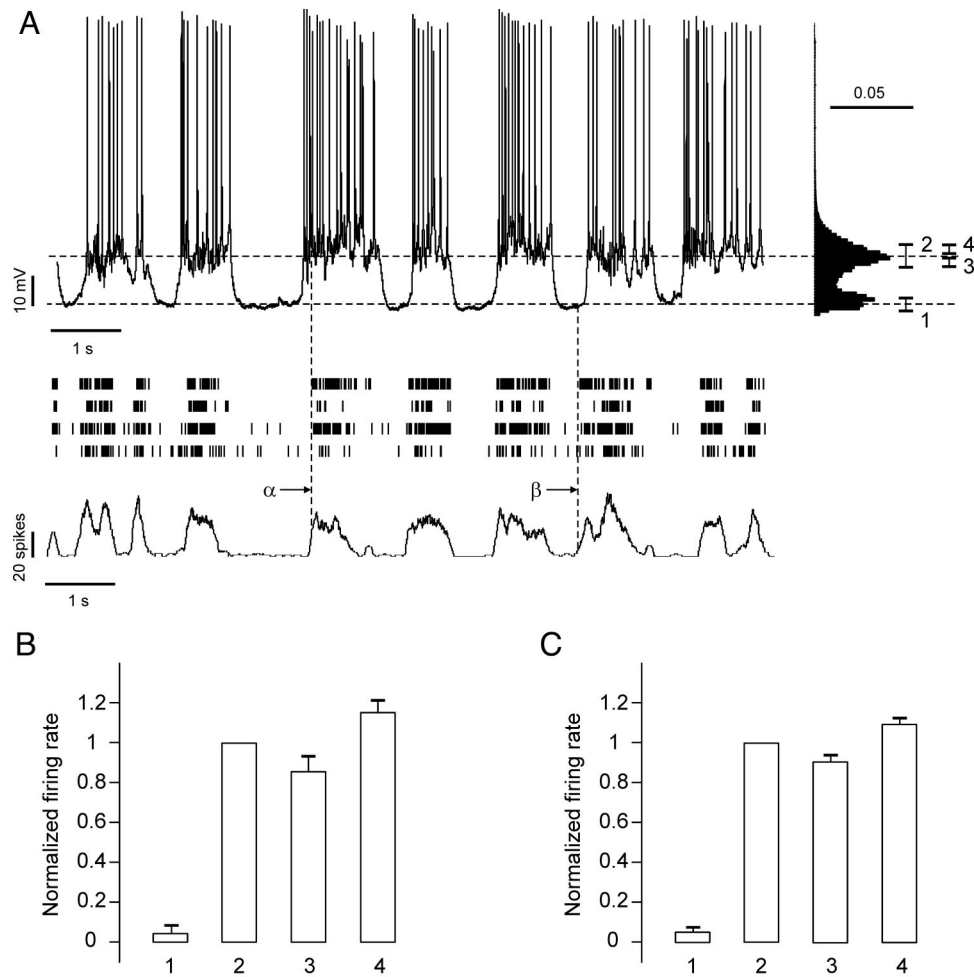


FIG. 1. Extracellularly measured network activity increases coherently during periods associated with depolarized membrane potential of intracellularly recorded neurons. *A*: example of simultaneous intracellular recording of a neuron together with several other neurons recorded extracellularly with 4 tetrodes inserted in close vicinity ( $<400 \mu\text{m}$ ). *Top*: 10 s of intracellular recording of a neocortical pyramidal neuron. *Middle*: 4 traces of simultaneous multiunit activity recorded by the 4 tetrodes. Each bar marks the time of occurrence of a spike detected with one of the tetrodes. *Bottom*: estimated network spike activity rate, computed by replacing each extracellular spike in the *middle traces* by a centered square pulse of amplitude one and duration of 100 ms. Note that the extracellularly recorded neurons alternate between periods of high and low activity, in phase with the “up” and “down” states of the intracellularly recorded neuron. Intra- and extracellular fluctuations are, however, imperfectly synchronized because the extracellular packet of activity arrives sometimes later (instance  $\alpha$ ) or earlier (instance  $\beta$ ) than the beginning of an intracellular “up” state. *Right*: amplitude probability distribution of the 10 s of intracellular membrane potential shown on the *left*. Bimodality of this distribution reflects the “up” and “down” states. Four membrane potential intervals are defined to compare periods when the intracellularly recorded neuron resides in a “down” state (1), an “up” state (2), or in the lower half (3) or upper half (4) of the “up” state. Widths of intervals 2, 3, and 4 are always fixed at 8, 4, and 4 mV, respectively, to allow for comparison between different cells. *B*: bar plot of the average extracellular firing rate when the membrane potential of the intracellularly recorded neuron shown in *A* resides in the intervals 1, 2, 3, or 4. Firing rates are normalized to the average firing rate in the “up” state (interval 2). Error bars show the SE for 10 successive evaluations of the firing rates, made on 100-s-long measurements of spontaneous activity. *C*: measurements presented in *B* were repeated and averaged for all intracellularly recorded cells in this first series of experiments ( $n = 6$ ). Error bars show SE for these 6 experiments.

intracortical microstimulation through 2 bipolar electrodes, placed around the intracellularly recorded neuron, was used to study how paired stimuli, presented at different time delays, are integrated by the neuron.

### Surgery

The experiments were performed on 25 Sprague–Dawley or Long–Evans rats (190–440 g body weight). Animals were initially anesthetized with urethane (1.0 g per kg body weight, intraperitoneally [ip]), and given supplemental injections of ketamine–xylazine as needed (20 mg per kg and 2 mg per kg, respectively, ip). The animal’s body temperature was maintained at 37°C. The animal was placed in a stereotaxic instrument, and the skull exposed with a single incision. In some cases, when recordings were not stable or showed heartbeat or breathing artifacts, the cisterna magna was opened to relieve intracranial pressure. All animals continued to breathe without artificial

respiration and were suspended by a clamp at the base of the tail to minimize movements of the brain caused by breathing. For insertion of the recording and stimulating electrodes in the frontal cortex, a round opening of about 3–5 mm in diameter was made in the skull, with the center about 3–4 mm anterior to bregma and the same distance lateral to the midline.

### Simultaneous intra- and extracellular recordings

Intracellular recordings were performed using sharp glass micropipettes, filled with 1 M potassium acetate. Electrode resistances ranged from 80 to 150 M $\Omega$ . Recordings were made with a bridge amplifier (SEC-05L, npi electronic GmbH, Tamm, Germany) and low-pass filtered at 5 kHz. Extracellular recordings of neuronal activity were performed using tetrodes made of NiCr wires (10  $\mu\text{m}$  diameter, Isabellenhütte, Heusler, GmbH KG, Dillenburg, Germany), coated

with Pt to achieve an electrode resistance of 500 k $\Omega$ . Extracellular signals were amplified 5,000 times, band-pass filtered (1 Hz to 5 kHz), and sampled at 50 kHz together with the intracellular signal using a Multi Channel System (MCS GmbH, Reutlingen, Germany) data-acquisition system. Four tetrodes were inserted about 0.5 to 1 mm deep into the cortex at the corners of a 550- $\mu$ m-side square. The intracellular electrode was inserted in the center of this square, at about 400  $\mu$ m from each tetrode. After insertion of both types of electrodes, the exposed cortex was covered with a low-melting-point paraffin wax to reduce brain pulsations. After digital filtering, spikes were detected on extracellular signals using a simple threshold criterion (Matlab, The MathWorks, Natick, MA). No attempt was made to achieve spike sorting because network activity could be estimated simply from the multiunit activity.

### Intracellular recordings with intracortical stimulation

Four stimulating electrodes (tapered tungsten wire) were inserted about 1 mm deep into the cortex. Their tips had fixed distances, being located on the corners of a rectangle measuring 1.0  $\times$  0.14 mm. The intracellular recording electrode was inserted near the center of this rectangle. For microstimulation we chose the 2 stimulating electrodes that most effectively (least stimulus current) elicited PSPs in the intracellularly recorded neuron. The remaining 2 were used as reference electrodes to achieve bipolar stimulation. Currents were delivered from stimulus isolation units (WPI, A360). Stimulus current amplitudes were adjusted such that a PSP elicited during a quiescent state reached a peak depolarizing amplitude of 1–3 mV. Across all experiments, the current amplitudes used were between 35 and 100  $\mu$ A. Duration of current flow was 100  $\mu$ s. Microstimulation was

computer controlled using LabVIEW (National Instruments). The membrane potential of the recorded neuron was analyzed on-line to detect transitions between “up” and “down” states. Two thresholds were used to detect the transitions: one for the down-to-up transitions at about 5 mV above the average “down” state potential and one for the up-to-down transitions at about 10 mV below the average “up” state potential. These transitions were used to trigger the stimuli, which were timed to occur either at a delay of 200 ms to stimulate during states (Figs. 2 and 4), or at a delay of only 10 ms when stimulating during state transitions (Fig. 6). A series of stimuli consisted of single and paired stimuli with various delays: 0.2, 1.0, 5.0, 10.0, 20.0, and 50.0 ms, with an interstimulus interval of 5 s. We did not use perfectly synchronized stimuli with  $\Delta t = 0$ , to avoid possible nonlinear effects attributed to activation of tissue located between both stimulating sites, which would not respond to either stimulus alone but possibly to a combination of both. With the time constants of excitatory synaptic currents in cortical neurons being in the range of milliseconds (Hestrin 1993), we considered a delay of 200  $\mu$ s between 2 consecutive stimuli as equivalent to “synchronous.”

Detection of transitions between the two states was also used in the experiment shown in Fig. 5. After a transition to the “down” state, a DC current (0.2 to 0.5 nA) was injected to depolarize the membrane potential to the typical “up” state value. Microstimulation during these periods of membrane depolarization was used to measure the effect of voltage change alone on PSP shape.

To measure membrane resistance and time constant, hyperpolarizing currents of 0.1 nA (100 ms) were injected every 250 ms during both “up” and “down” states (Fig. 3). Membrane resistance was estimated from the amplitude of the voltage response and membrane time constant from its decay time (first-order exponential fit).

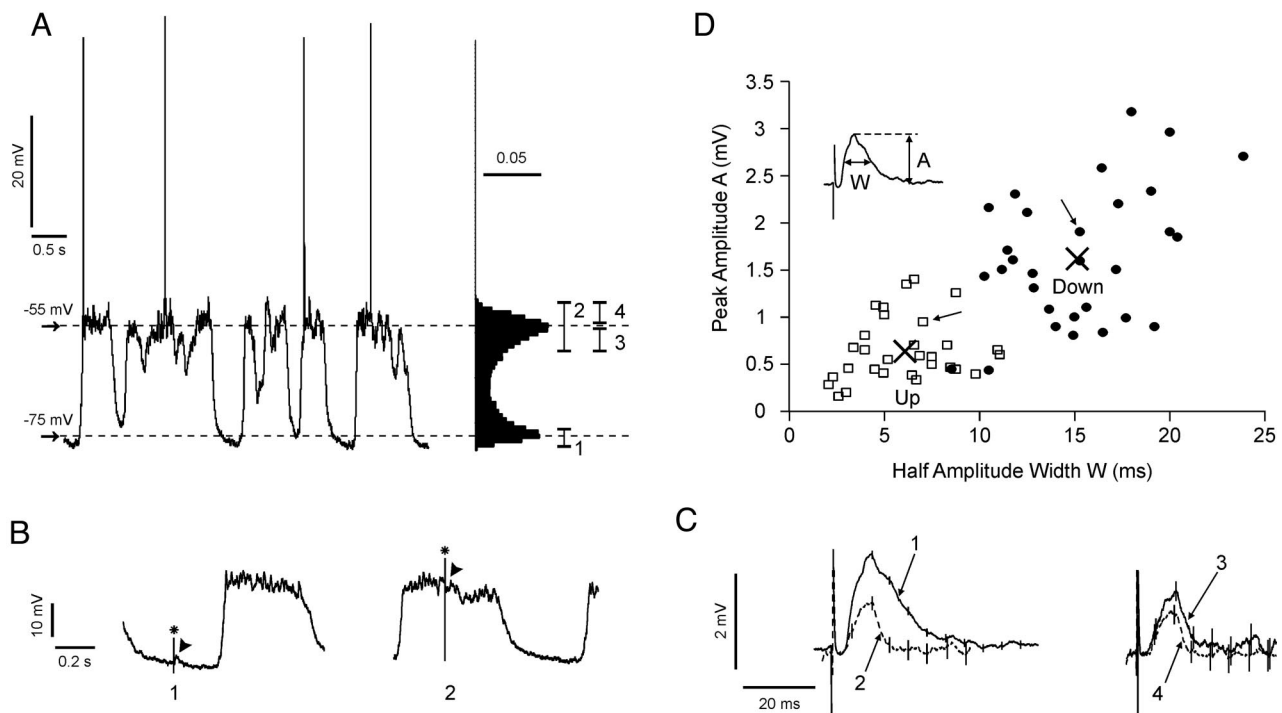


FIG. 2. Shape of postsynaptic potentials (PSPs) strongly depends on the state and depolarization level of the neuron at the time of stimulation. *A: Left:* 10 s of spontaneous activity from an intracellularly recorded neocortical pyramidal neuron. *Right:* amplitude probability distribution of the intracellular membrane potential shown on the left. Intervals 1, 2, 3, and 4 as defined in Fig. 1A. *B:* effect of a single electrical stimulus during a “down” state (left) and an “up” state (right) period (stimulus artifacts marked by asterisks). Stimulus-induced postsynaptic responses are marked by arrowheads. *C:* comparison between averaged postsynaptic responses to stimuli elicited during “down” states (1) and “up” states (2) (left,  $n = 60$  repetitions each), and during the lower (3) and the upper (4) halves of the “up” states (right,  $n = 25$  repetitions each). Vertical bars along the averaged PSP traces indicate the SE. *D:* peak amplitude of the averaged PSPs as a function of their width at half-amplitude for all 30 recorded pyramidal cells. Filled circles and the open squares indicate PSPs elicited during “down” and “up” states, respectively. Two large crosses indicate the mean positions of “up” and “down” state distributions. Two arrows point to the values obtained for the cell shown in A–C. *Inset:* definition of the peak amplitude (A) and width at half-amplitude (W) of PSPs.

### Histology and cell identification

According to physiological and/or histological criteria and the penetration depth of the electrode, cells recorded in this study were pyramidal cells from all cortical layers. Cell types were assessed using the electrophysiological measurement of spike duration: all cells used in this study produced spikes with half-amplitude duration larger than 1.5 ms, corresponding to pyramidal neurons. Additionally, in several experiments, the intracellular electrode also contained 4% neurobiotin

(Vector Laboratories, Burlingame, CA) for visualization and histological verification. To fill cells with neurobiotin, depolarizing current pulses (1 nA, 500 ms, 1 Hz) were passed through the electrode for 10 min at the end of the experiment. After a recording session, the animals were injected with a urethane overdose and then perfused intracardially with 500 ml physiological saline followed by 500 ml of 4% paraformaldehyde in phosphate-buffered saline. The brains were removed and stored in fixative solution overnight. Frontal sections (200  $\mu\text{m}$ ) were cut and processed for neurobiotin labeling (ABC Elite Kit, Vector Labs).

### Data analysis

Neurons that had membrane potentials of  $-60$  mV or more negative during the quiescent state and spikes with peak amplitudes more positive than 0 mV were included in the analysis.

**SUMMATION IN “UP” AND “DOWN” STATES.** Data were analyzed using Matlab (The MathWorks). PSPs arriving during the quiescent or depolarized states were grouped according to state and stimulus pattern, and the averages and SE values were calculated. Discrimination between quiescent (“down”) and depolarized (“up”) state was based on the mean and variance of the membrane potential distribution immediately before and after the PSPs. Responses to stimulation with each single electrode alone were grouped accordingly, and the data traces were used to calculate mean and SE of the linear expectation of the response waveform. To this end they were systematically shifted over time relative to each other, corresponding to the temporal delays used in the experiment. Thus for each of  $N$  pairs of single-electrode response waveforms [responses to stimulation with electrode 1 =  $x_{1(1..N)}$  and with electrode 2 =  $x_{2(1..N)}$ ], the algebraic sums ( $x_{1i} + x_{2i}^{\Delta t}$ ) were calculated for each time delay ( $\Delta t$ ). The mean linear predictor ( $\bar{x}_{1,2}^{\Delta t}$ ) for each delay ( $\Delta t$ ) and the resulting SE value ( $S_M^{\Delta t}$ ) were then calculated in the standard fashion.

**SPIKE GENERATION PROBABILITY.** We calculated the probability of obtaining at least  $n$  excess input spikes by chance within a certain time window, assuming 10,000 independent Poissonian inputs with a rate of 4.5 spikes/s each. (Statistical analysis of our recordings of spontaneous spiking activity during the “up” state had revealed an average firing rate of 4.5 spikes/s over the recorded population of neurons ( $n = 30$ ), with close to exponential interval distributions [not shown].) During a time window of  $\Delta t = 10$  ms, the average number of synaptic inputs received by such a neuron is  $N = 450$ . The probability of obtaining an excess of at least  $n = 60$  inputs during  $\Delta t$  was calculated by summing the probabilities to obtain the counts  $N + n, N + n + 1, N + n + 2, \dots$  for a Poissonian process with a mean count of  $N$

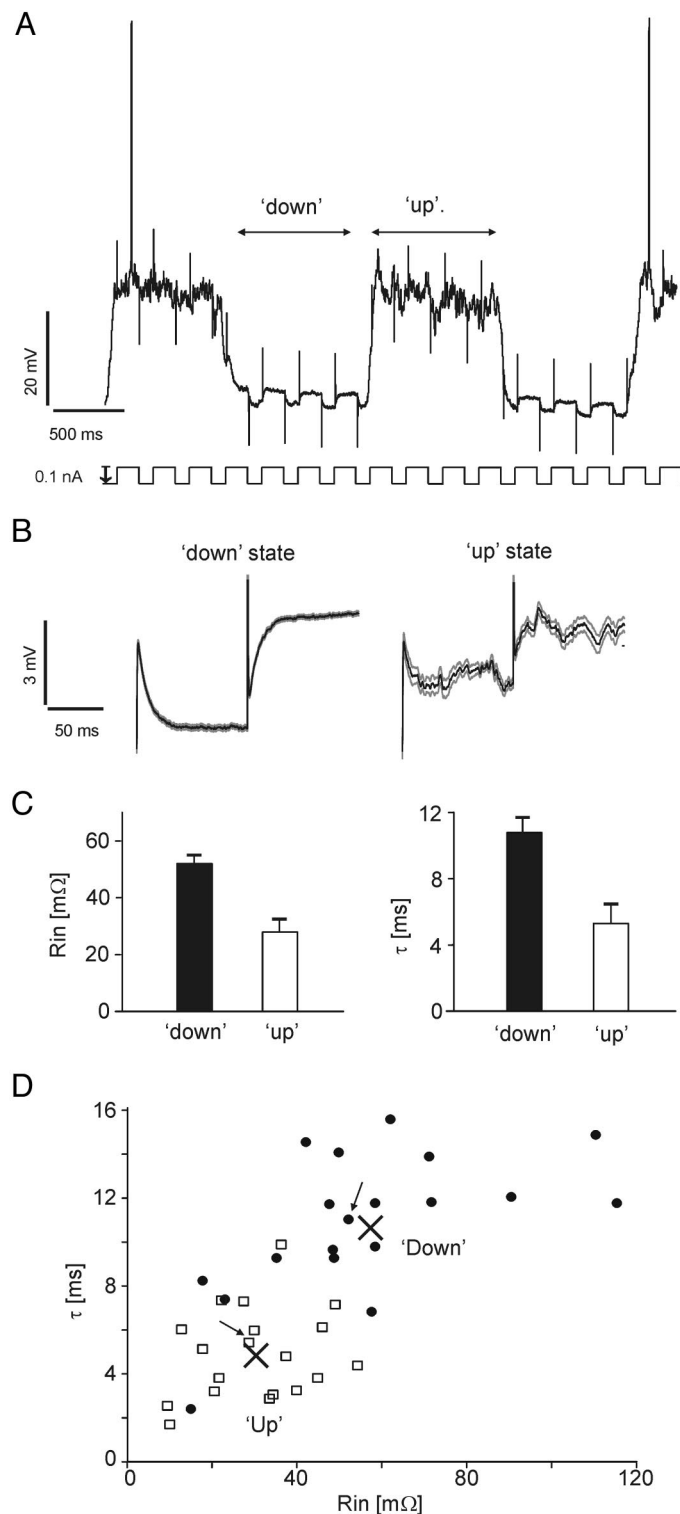


FIG. 3. Neuronal input resistance  $R_{in}$  and time constant  $\tau$  as a function of membrane potential state. *A*: hyperpolarizing current pulses of 0.1 nA and 100-ms duration (bottom) were injected into the neuron every 250 ms. Voltage deflections (top) recorded during “up” and “down” states were analyzed separately. *B*: average voltage response recorded during “down” (left) and “up” (right) states for the neuron shown in Fig. 2. Black and gray traces represent mean and SE, respectively ( $n = 100$  pulses). Dashed traces show first-order exponential fits. *C*: during “down” and “up” states, input resistance  $R_{in}$  (left) was estimated from the amplitude of the voltage response shown in *B*, and time constant  $\tau$  (right) from its decay time. Bar graph in *C* presents the results for  $R_{in}$  and  $\tau$  obtained for the neuron shown in Fig. 2. Error bars mark 95% confidence interval. *D*: scatter plot of the time constant vs. input resistance measured for all 19 cells used for the cell parameter analysis. Filled circles and the open squares indicate  $R_{in}$  and  $\tau$  measured during “down” and “up” states, respectively. Two large crosses indicate mean values of the “up” and “down” state distributions (“down” state:  $R_{in} = 56.9 \pm 6.2$  M $\Omega$  [mean  $\pm$  SE],  $\tau = 10.7 \pm 0.7$  ms; “up” state:  $R_{in} = 30.4 \pm 3.0$  M $\Omega$ ,  $\tau = 4.9 \pm 0.5$  ms;  $n = 19$  cells). Two arrows point at the values obtained for the cell shown in Fig. 2 and Fig. 3, A–C.

$$P = \sum_{i=N+n}^{\infty} \frac{N^i}{i!} e^{-N}$$

## RESULTS

*Temporal relationship between network activity and membrane potential fluctuations*

Intracellular recordings were obtained from frontal cortex pyramidal neurons of anesthetized rats. In a first series of experiments, simultaneous multiunit activity was recorded from extracellular electrodes (tetrodes) placed in the close vicinity of the intracellular electrode (<400  $\mu\text{m}$ ). This combination of intra- and extracellular electrodes allows determination of the temporal relationship between the membrane potential fluctuations of a single pyramidal neuron and the spike activity in its surrounding network. In this study, 6 cells were recorded intracellularly together with network activity using this method. A typical simultaneous recording is presented in Fig. 1A. The *top trace* shows the typical membrane potential fluctuations with hyperpolarized, quiescent periods alternating with depolarized periods with large voltage fluctuations and spike activity. Neocortical pyramidal neurons are known to exhibit these membrane potential fluctuations—commonly referred to as “up” and “down” states (Cowan and Wilson 1994; Steriade et al. 1993)—under urethane and ketamine/xylazine anesthesia. *Middle traces* in Fig. 1A show the spike times detected on the 4 tetrodes. Observe that multiunit spikes occur in clusters, coinciding with the occurrence of the intracellular “up” states; this is quantified by comparing the average extracellular firing rates, whereas the intracellularly recorded neuron resided in the “down” state (Fig. 1, *B* and *C*, *column 1*) or in the “up” state (Figs. 1, *B* and *C*, *column 2*). Note also, however, that the spike packets visible by grouping spikes detected on all 4 tetrodes (Fig. 1A, *bottom trace*) do not perfectly time-lock with the intracellular “up” states. Their beginning can sometimes follow (Fig. 1A, instance  $\alpha$ ) or precede (Fig. 1A, instance  $\beta$ ) the initiation of an intracellular “up” state. A detailed examination of the synchronization between intracellular and extracellular patterns is presented later (Fig. 7). At this stage, however, it can already be concluded that the intracellularly observed “up” and “down” membrane fluctuation states are to a large extent concomitant with periods of high and low activity in the surrounding network (see also Amzica and Steriade 1995; Stern et al. 1997). This conclusion is in accordance with previous work, showing with dual intracellular recordings that “up” and “down” states among cortical neurons are synchronized (Contreras and Steriade 1995; Steriade et al. 1998).

The advantage of using several extracellular electrodes, instead of a second intracellular electrode, to detect activity in the surrounding network is that it allows for the simultaneous observation of a larger fraction of the network. In the example shown in Fig. 1A, the overall extracellular firing rate among all 4 tetrodes is 164 spikes/s. Assuming that firing rates of individual frontal cortex neurons range between 0.5 and 20 spikes/s, the 4 tetrodes in this case recorded altogether from about 10 to 300 neurons. This provides enough spikes from the surrounding network to evaluate how its activity relates to the single neuron’s membrane potential fluctuations, not only to

the large “down” to “up” and “up” to “down” state transitions, but also to the finer fluctuations within the “up” state. To this end, we divided the membrane potential levels corresponding to the “up” states into 2 equal subintervals, the upper and the lower halves (called intervals 3 and 4, respectively, in the distribution of membrane potential values shown in the *right-hand part* of Fig. 1A). Accordingly, we determined the average firing rate of the observed fraction of the surrounding network while the neuron’s membrane potential resided within each of these subintervals. Figure 1, *B* and *C* show that, on average, the network activity remained lower while the membrane potential was in the lower half of the “up” state, and increased when the membrane potential dwelled in the upper half of the “up” state (in the lower half, the network firing rate reached  $90.5 \pm 2.7\%$  of its average level during the “up” state, and  $109.4 \pm 2.8\%$  in the upper half,  $n = 6$ ; Fig. 1C).

In summary, these simultaneous intra- and extracellular recordings reveal that the pattern of membrane potential fluctuations exhibited by frontal cortex pyramidal neurons is closely related to modulations of the activity level in the surrounding network. “Down”-state regimes correspond to periods of a quasi-silent network and are interrupted by epochs with intensive spiking events in the network, coinciding with “up”-state regimes. Moreover, as the strength of these network discharges increases, the membrane potential during “up” states is, on average, more depolarized.

*Stimulated inputs at different levels of network activity*

In a second series of experiments we compared the effect of stimulated inputs on the membrane potential of an intracellularly recorded neuron, while it experienced different regimes of network activity (Fig. 2). Subthreshold depolarizing PSPs were elicited by electrically stimulating fibers (Nowak and Bullier 1998a,b) at sites  $\leq 500 \mu\text{m}$  from the recorded neuron. We used 2 bipolar stimulating electrodes placed about 1 mm deep into the cortex. Stimulation was applied during both the “down” (Fig. 2B, *left*) and the “up” states (Fig. 2B, *right*). To keep PSPs subthreshold in all conditions, current strength was adjusted such that depolarizing PSPs in response to stimuli during the “down” state typically had amplitudes of 1 to 3 mV. Because of the stationarity of the hyperpolarized membrane potential in the “down” state, PSPs were clearly visible during each single trial. However, when the same stimulus was used to stimulate inputs during an “up” state, the induced PSP remained mostly undetectable in the strong membrane potential fluctuations (Fig. 2B, *right*). Thus an average over several trials was first required to compare responses in these different regimes. We first compared averaged PSPs induced during either “down” or “up” states (Fig. 2C, *left*) because these regimes corresponded to strongly contrasting network activity levels (Fig. 1). The resulting averaged PSP shapes showed two striking differences: both the amplitude of the PSP and its duration were markedly reduced in the “up” state as compared with the “down” state. Across all 30 cells recorded in this second series of experiments, the reduction of peak amplitude reached a factor of  $2.8 \pm 0.6$ , and the reduction of PSP duration at half-amplitude amounted to a factor of  $2.9 \pm 0.8$  (Fig. 2D). Note that the time to peak of PSPs was identical in the “up” and “down” states ( $7.7 \pm 1.1$  ms in the “down” state,  $7.6 \pm 1.2$  ms

in the “up” state,  $n = 30$  cells) and thus only the difference in decay phase of PSPs contributed to the change of PSP duration.

As described above, the network activity during the “up” state is not constant: as the network activity increases, the membrane potential during “up” states is, on average, more depolarized (Fig. 1). To investigate the effect of the associated fluctuations of network activity on PSPs, we grouped together trials in which PSPs were induced during either of the 2 subregimes of the “up” state (intervals 3 and 4 in Fig. 1), and compared the averaged PSP shapes for these 2 groups (Fig. 2C, right). PSPs occurring during the upper half of the “up” state were smaller in amplitude by a factor of  $1.5 \pm 0.4$ , and shorter in duration by a factor of  $1.4 \pm 0.4$  than PSPs occurring during the lower half (Fig. 2C, right,  $n = 30$  cells). Taken together, these findings indicate that PSP size and duration are strongly modulated by the level of the membrane potential and/or by the associated level of ongoing activity in the surrounding network, with higher membrane potential (network activity) resulting in markedly smaller and shorter PSPs.

#### *Cell parameters at different levels of network activity*

Earlier findings in anesthetized cats (Borg-Graham et al. 1998; Contreras et al. 1996; Paré et al. 1998) have shown that the cell’s input resistance ( $R_{in}$ ) and time constant ( $\tau$ ) are decreased during the “up” state. This is likely attributable to the opening of large numbers of ligand-gated ion channels by incoming synaptic activity. On the basis of theoretical studies (Bernander et al. 1991; Destexhe and Paré, 1999; Rapp et al. 1992) it has been predicted that such changes of  $R_{in}$  and  $\tau$  would have a strong influence on the amplitude and duration of PSPs. To evaluate whether this mechanism would be in effect in our preparation, we quantified the input resistance under different levels of network activity. Thus  $R_{in}$  and  $\tau$  were measured in both states by repetitively injecting small hyperpolarizing current steps (Fig. 3). On average, both  $R_{in}$  and  $\tau$  decreased by a factor of about 2 from the “down” to the “up” state ( $R_{in}$ :  $1.87 \pm 0.39$ ,  $\tau$ :  $2.21 \pm 0.36$ ;  $n = 19$  cells; Fig. 3D). These results are in accordance with the earlier findings in cats. They suggest that a mechanism based on the modification of  $R_{in}$  and  $\tau$  by network activity can indeed contribute to the decrease in PSP amplitude and duration observed in our experiments.

#### *Presence of inhibitory components in the evoked response*

Another mechanism that could play a role in the decrease in amplitude and duration of the PSPs in the “up” state is the presence of inhibitory postsynaptic potentials (IPSPs) in the evoked response to stimulation in the “up” state. Because the reversal potential of IPSPs is close in voltage to the membrane potential level attained in the “up” state (indirect measurements from Cowan and Wilson 1994), such inhibitory components are difficult to observe. Even if it is not clearly visible in the example shown in Fig. 2, we indeed found certain stimulation settings where inhibitory components were visible in the “up” state response (see responses to paired stimuli with delays of 5 and 10 ms in Fig. 4A).

#### *Input summation at different levels of network activity*

Input summation occurs when independently arriving PSPs overlap in time. Because PSP duration varies with the level of

network activity, it follows that the window for temporal integration of synaptic inputs should be resized accordingly. To test this hypothesis, we inserted two bipolar stimulating electrodes close to the intracellular recording electrode, one on each side, and compared how 2 packets of synaptic inputs elicited by these stimulating electrodes were summated during different regimes of network activity. Stimuli were first delivered from each of the 2 cortical sites individually, and then from both together, but with varying time delay ( $\Delta t$ ), ranging from 0.2 to 50 ms, in between. Trials were separated by 5 s. Typical examples of averaged traces of resulting compound PSPs are shown in Fig. 4A (black traces) for the same neuron as in Fig. 2. Stimulations occurring during “up” and “down” states were averaged separately to allow for a comparison between regimes with distinct levels of network activity. Red traces in Fig. 4A correspond to linear predictors, computed by summing the appropriately time-shifted responses to the individual stimuli (see METHODS). Among all cells recorded and analyzed ( $n = 30$ ), the deviation from linearity never exceeded 20% of the PSPs peak amplitudes (Fig. 4D). In particular, we found no systematic nonlinear behavior for coincident inputs (i.e.,  $\Delta t = 0.2$  ms), neither in the “down” state nor in the “up” state. Moreover, the response to the first stimulus had no effect on the amplitude or the shape of the response to the second stimulus, thereby effectively limiting the time window of synaptic integration to the duration of the PSP. Figure 4B shows the peak amplitudes for all conditions shown in Fig. 4A. This graph summarizes the 3 principal findings of the second series of experiments: 1) summation of PSPs in the frontal cortex is essentially linear; 2) the amplitude of the neurons’ response in the “up” state is less than half that in the “down” state; 3) the time window during which 2 PSPs summate is shortened by a factor of more than 2 from “down” to “up” state. Together with the results of Figs. 1C and 2C, these findings indicate that the time window for synaptic integration is reduced in proportion to the level of background network activity.

#### *Are PSPs shaped by network activity or by voltage-dependent mechanisms?*

The regimes of intracellularly measured membrane potentials analyzed in our study (the “up” and “down” states, the upper and lower halves of the “up” state) differ not only in their averaged somatic membrane potential levels, but also in the associated levels of network activity. Therefore additional experiments were carried out to determine to what extent PSP shape modulations resulted from mechanisms depending on the membrane potential per se.

In a first approach, somatic current injection (0.2 to 0.5 nA) was used to raise the membrane potential during a “down” state to the level of the “up” state (Fig. 5A). We found that stimulus-induced PSPs arriving during current injection had the shape of “down”-state PSPs, except for a  $20 \pm 6\%$  ( $n = 10$  cells) reduction in peak amplitude (Fig. 5B). The PSPs amplitude in the “up” state was still  $47 \pm 5\%$  (Fig. 5C,  $n = 10$  cells) smaller. The comparison of these results indicates that non-voltage-dependent mechanisms significantly contribute to the amplitude reduction in the “up” state. However, an important limitation of this approach resides in the difficulty to quantitatively assess the space-clamp quality of the recorded neuron.

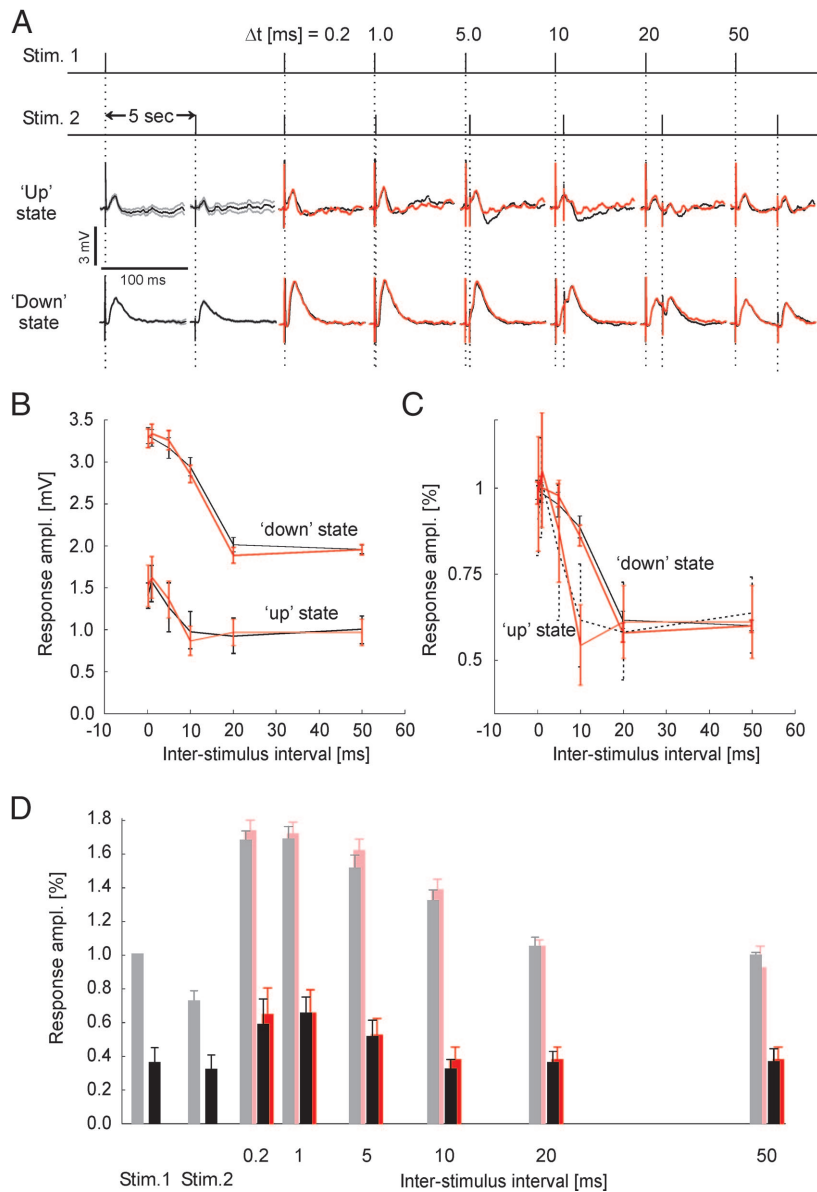


FIG. 4. Summation of PSPs is linear in both “up” and “down” states. *A*: stimulus protocol consisted of a set of 8 different stimuli presented at intervals of 5 s. *First row from top*: (Stim. 1) stimulation at site 1. *Second row (Stim. 2)*: stimulation at site 2. *Third and fourth rows*: black and gray traces: subthreshold responses to stimulation at each individual site (black = mean, gray = SE,  $n = 60$  repetitions) during the “up” and “down” states. Black and red traces represent the average measured response (black) to paired stimulation and the linear predictor (red) calculated from the responses to the individual stimuli. Slight hyperpolarization (black) sometimes seen in response to the stimulus in the “up” state (responses to paired stimuli with delays of 5 and 10 ms in the example shown here) could be attributable to an inhibitory component of the neuronal response (see DISCUSSION). *B*: peak amplitude of responses, presented in *A*, as a function of stimulus delay, both in the “up” and “down” states. Black = measured, red = linear predictor. Error bars mark SE. *C*: same data as in *B*, but normalized to the peak amplitude response obtained at stimulus delay of 0.2 ms. Note the reduction of the window for effective summation in the “up” state compared with the “down” state. Data shown in this figure were obtained from the same neuron as in Fig. 2. *D*: averaged peak amplitudes of responses as a function of stimulus delay for all 30 cells used in this analysis. To allow for comparison between all cells, data are systematically normalized to the peak amplitude of the largest stimulus response obtained in the “down” state. Gray bars: measured amplitudes in the “down” states; black bars: measured amplitudes in the “up” states; pink bars: linear predictor in the “down” state; red bars: linear predictor in the “up” state. Stim. 1 and Stim. 2 are the average responses elicited by each stimulus alone. Error bars mark SE,  $n = 30$  cells.

Because the space clamp of the neuron is likely to be restricted to the soma and its vicinity (Spruston et al. 1994), this experiment is particularly relevant for the fraction of the stimuli passed to the neuron through proximal synapses.

In a second approach to distinguish between purely voltage dependent or network activity–dependent mechanisms, we stimulated synaptic inputs to arrive at identical membrane potential levels during the transitions between “up” and “down” states. As we will show later (Fig. 7), the two types of transitions (from “down”-to-“up” and from “up”-to-“down” states) are associated with different dynamics of network activity changes. As a consequence, at the time the somatic membrane potential reaches the midtransition value—which is the same in both types of transition—the level of network activity during “down” to “up” transitions is significantly higher than that during “up” to “down” transitions (cf. Fig. 7A). Thus if stimulus-induced PSPs arriving in these 2 configurations would be identical, this would strongly argue in favor of purely voltage dependent mechanisms. If, on the other hand,

the stimulus-induced PSPs would be different, this would equally strongly argue against purely voltage dependent mechanisms.

Thus presynaptic fibers were stimulated during transitions between states. Two independent voltage thresholds were used to detect transitions and to trigger stimuli. Trigger levels and stimulus delays were adjusted such that the stimulus-induced PSP arrived at the time when the membrane potential value was halfway (midtransition) between “down” and “up” states (Fig. 6, *A* and *B*). Figure 6C illustrates the averaged response of a neuron to these stimulations during transitions. PSPs arriving at “down”-to-“up” (“up”-to-“down”) midtransition—and thus during high (low) network activity—had the size and shape of the “up” (“down”) state PSPs (Fig. 6D). These results, in line with our earlier findings, support the hypothesis that PSPs are shaped by network activity, independent of somatic membrane potential.

To quantify the dynamic changes of network activity during the membrane potential state transitions, we reanalyzed the data from

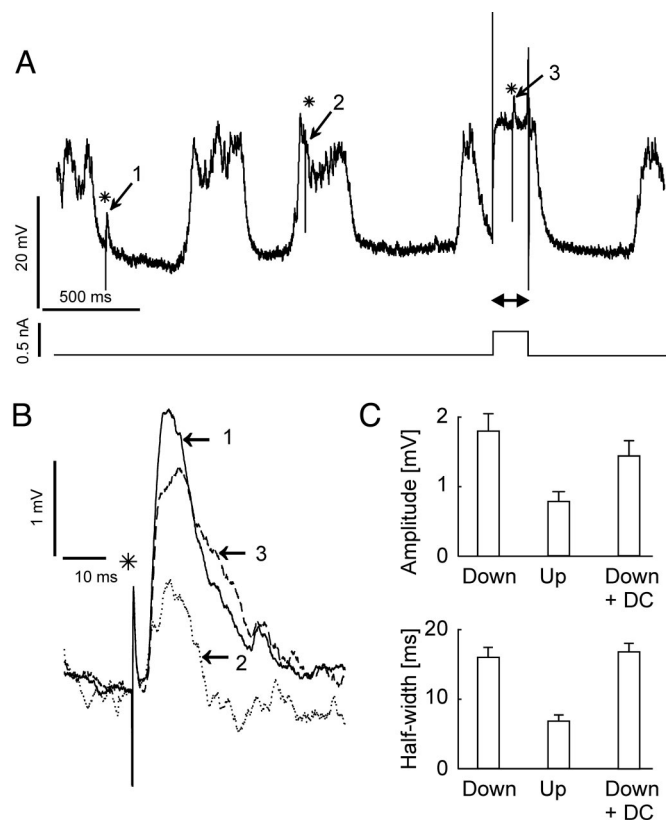


FIG. 5. Influence of membrane potential level on PSP shape. *A*: using one stimulating electrode, PSPs were elicited during “down” states (1), during “up” states (2), and, finally, during “down” states in which the neuron was depolarized by somatic injection of a DC current, raising the membrane potential to a typical “up” state value (3). Horizontal arrow marks the period of DC current injection. *B*: comparison between the averaged PSP traces in these 3 conditions ( $n = 50$  repetitions in each condition). Raising the membrane potential to “up”-state values during the “down” state decreased PSP amplitudes by about 20%, as expected because of the reduced driving force, but did not reduce PSP duration. *C*: mean response peak amplitudes (top) and half-amplitude width (bottom) averaged across all cells tested in these 3 configurations. Error bars mark SE,  $n = 10$  cells.

the simultaneous intra- and extracellular recordings described in Fig. 1. The detailed temporal relationship between intra- and extracellular activity dynamics was measured by calculating the histogram of extracellular spikes, triggered on the times of intracellular midtransition. Figure 7A shows the comparison between averaged transition profiles of the neuron membrane potential and the concurrent changes of network activity for “down”-to-“up” (left) and “up”-to-“down” (right) transitions. Observe that the average network activity level at the time of midtransition is clearly higher in the upward than in the downward transition (“down”-to-“up”:  $81.4 \pm 2.7\%$  of reference “up” state level; “up”-to-“down”:  $26.7 \pm 9.2\%$ ;  $n = 6$ ; Fig. 7A).

Taken together, the difference in size and duration of PSPs elicited at both types of midtransitions and the difference in the concurrent network activity levels indicate that the principal cause for PSP modulations is not simply a voltage-dependent mechanism, but rather likely one or several mechanisms depending on the network activity level.

#### Synchronization of inputs and spike generation

The mechanisms of PSP integration influence how the neuron is brought to produce a spike. With a temporal window for

synaptic integration all the more shortened as the membrane potential is depolarized, a neuron is required to receive many inputs in the last 10 ms (i.e., the reduced duration of PSPs during the “up” state) preceding spike onset to be able to reach its spike threshold. To quantify the time course of depolarization leading to the action potential, we computed spike-triggered averages of the membrane potential trajectories around the time of spike generation (Fig. 8). Note that one PSP duration (i.e., 10 ms) before spike onset (cf. legend of Fig. 8 for definition of spike onset), the membrane potential is on average still almost 5 mV below spike threshold, rising with a steadily increasing slope (Fig. 8C). The narrow width of the distribution of membrane potential trajectories for all spikes in the recording (Fig. 8D) indicates that this sharp increase is not just a property of the average (Fig. 8C), but a property of each individual spike (Fig. 8B). For the whole sample of cells analyzed in this study ( $n = 30$ ), the average difference between membrane voltage at 10 ms before spike onset and at spike threshold was  $4.7 \pm 0.5$  mV. Similar transient depolarizations leading to action potential firing have been reported for neurons in cat visual cortex in vivo (Azouz and Gray 1999). Such a short-lasting step of depolarization suggests that considerable synchronization among inputs is required to bring the neuron to fire a spike (see DISCUSSION).

#### DISCUSSION

We have explored here how background network activity in vivo influences the integration properties of cortical neurons. Our results enable us to draw 3 main conclusions. 1) Integration of separate inputs in frontal cortex neurons is linear, independent of synaptic delays and level of background activity. As a result, the time window for synaptic integration in cortical neurons in vivo is, in fact, limited by the duration of the PSPs, as had been suggested on theoretical grounds (Abeles 1982; Diesmann et al. 1999; König et al. 1996). 2) Both the duration and amplitude of PSPs are modulated by the level of background activity. Both are reduced by more than half during periods of high network activity (the “up” state) as compared with silent periods (the “down” state). Smaller changes in network activity within the “up” state exert a similar, but accordingly reduced, effect on PSPs. 3) Reductions of PSP size and duration are consistent with the concomitant decreases in input resistance and time constant caused by ongoing network activity (Fig. 3C). There are, however, other possible mechanisms that could affect PSP shapes in a similar way. Next, we will discuss these mechanisms and their possible contribution to PSP shape modulation.

#### Mechanisms for modulation of PSP shape

The reduction of PSP size and duration in the “up” state could in part be determined by purely voltage dependent mechanisms.

1) *The reduction in driving force.* The membrane potential in the “up” state is on average approximately 20 mV more depolarized than in the “down” state, thereby reducing the driving force for excitatory currents and thus decreasing their amplitude. This reduction in driving force alone, however, accounts for only at most a nearly 25% reduction of PSP amplitude (assuming a reversal potential for excitatory conductances close to 0 mV), and does not affect the duration of PSPs.

2) *Directly stimulated inhibition.* Intracortical microstimulation activates inhibitory as well as excitatory synaptic inputs

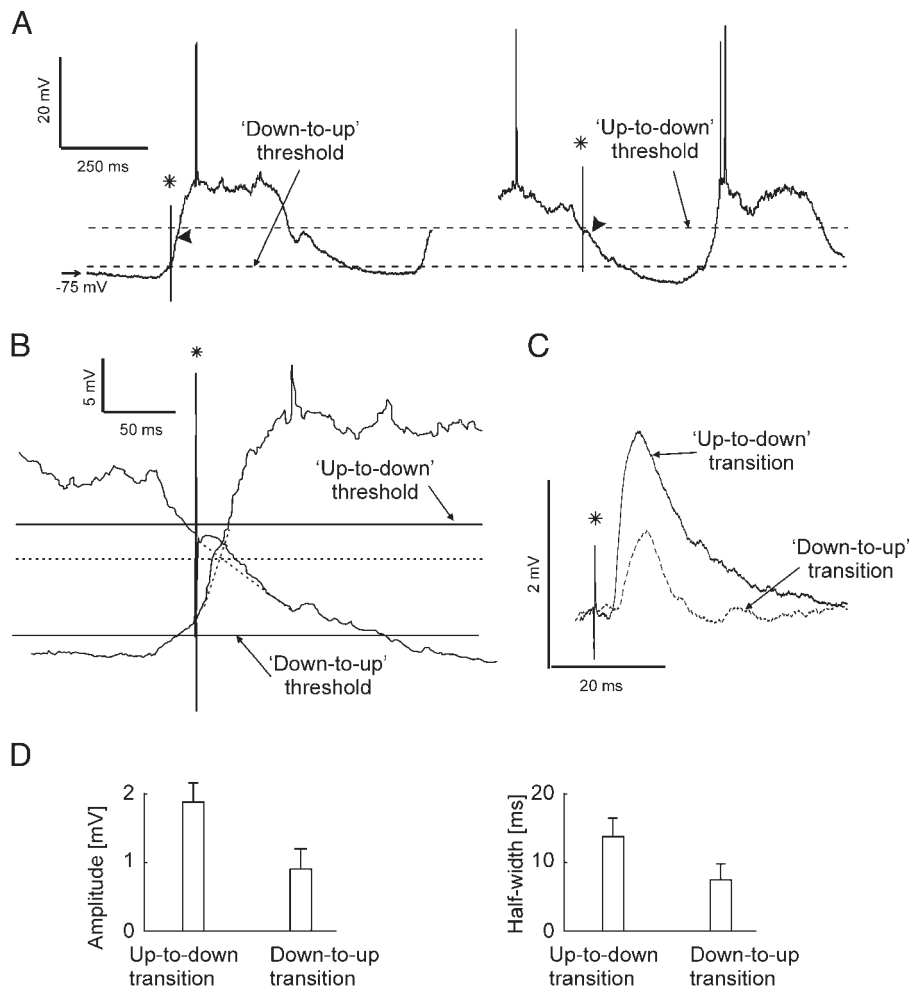


FIG. 6. Characteristics of PSPs elicited during "up" or "down" states are similar to those of PSPs elicited during the transitions toward these states. *A*: triggered-on transitions between states detected on-line using the 2 indicated thresholds (see METHODS); stimuli were delivered in relation to (see *B*) the times of midtransitions (stimulus artifacts marked by asterisks). Times of occurrence of stimulus-induced postsynaptic responses are marked by arrowheads. *B*: expanded view of the 2 superimposed examples of transitions shown in *A*, aligned on stimulus presentation time. Stimuli were delivered such that the PSPs had their maximum at the times when transitions reached their midway membrane potential level (oblique dashed lines crossing each other at the potential level marked by the horizontal dashed line). *C*: averaged PSP traces elicited during "falling" transitions from "up" to "down" states ( $n = 60$ ) and "rising" transitions from "down" to "up" states ( $n = 60$ ) are shown after a detrending procedure, which consisted in subtracting the respective averaged transition profiles. During a falling transition, PSPs are comparable to those obtained during the "down" state. By contrast, during a rising transition, PSPs are comparable to those obtained during the "up" state. Data shown in *A–C* were obtained from the same neuron as in Figs. 2 and 4. *D*: mean response peak amplitudes (left) and half-width (right) averaged across all the cells tested during the transitions between states. Error bars mark SE,  $n = 10$  cells.

to the intracellularly recorded neuron. Resulting PSPs can thus carry inhibitory components. Because the reversal potential of GABA<sub>A</sub>-mediated inhibition is between the average voltage levels of the "up" and "down" states (indirect measurements from Cowan and Wilson 1994), synchronous inhibitory input would tend to increase PSP amplitude in the "down" state, but decrease it in the "up" state.

3) *Voltage-gated (rectifying) currents.* Voltage-gated outward rectifying potassium currents activated by depolarization act to counterbalance further depolarization (Foehring and Surmeier 1993; Martina et al. 1998). Hyperpolarization-activated ( $I_h$ ) channels could act similarly: the deactivation of an  $I_h$  current by synaptic depolarization produces effectively a hyperpolarizing current during the "up" state, which could reduce PSP amplitude and duration (Magee 1999; Nicoll et al. 1993).

Each of these 3 voltage-dependent mechanisms could, in principle, contribute to the observed reduction of PSPs in the "up" state. However, the results of our experiments, especially those described in Figs. 5 to 7, indicate that they are not the principal cause for the PSP modulations we observed. Instead, our results point toward one or several mechanisms depending on the network activity level as being responsible for the observed modulation of the PSP shape.

1) *Modulation of the cell's input resistance ( $R_{in}$ ) and time constant ( $\tau$ ).* Our finding that, on average, both  $R_{in}$  and  $\tau$

decreased by a factor of close to 2 from the "down" to the "up" state (Fig. 3) indicates that the reduction of  $R_{in}$  with increased network activity accounts for most of the more than 2-fold decrease in PSP amplitude and duration.

2) *Indirectly stimulated inhibition.* Excitatory fibers activated by the intracortical microstimulation are likely to elicit excitatory postsynaptic potentials (EPSPs), not only in the intracellularly recorded pyramidal neuron, but in nearby inhibitory interneurons as well. "Up" and "down" states correspond to periods of high and low activity not only in pyramidal cells but also in inhibitory interneurons. These interneurons are more sensitive to stimulation in the "up" state than in the "down" state (Shu et al. 2003) (because they are more depolarized and thus more easily activated as a result of their electrical compactness), resulting in a more pronounced activation of the local inhibitory network in response to stimulation during the "up" state. With many of these interneurons likely to be connected to the intracellularly recorded neuron, this stronger activation of the local inhibitory network may introduce an inhibitory component to the stimulated inputs that is selectively more activated during "up" states than during "down" states, thereby contributing to the decrease in PSP amplitude and duration during periods of increased network activity. A related mechanism based on interneurons serving as relays to convey inhibition has recently been shown to shorten the temporal window for synaptic integration of hippocampal

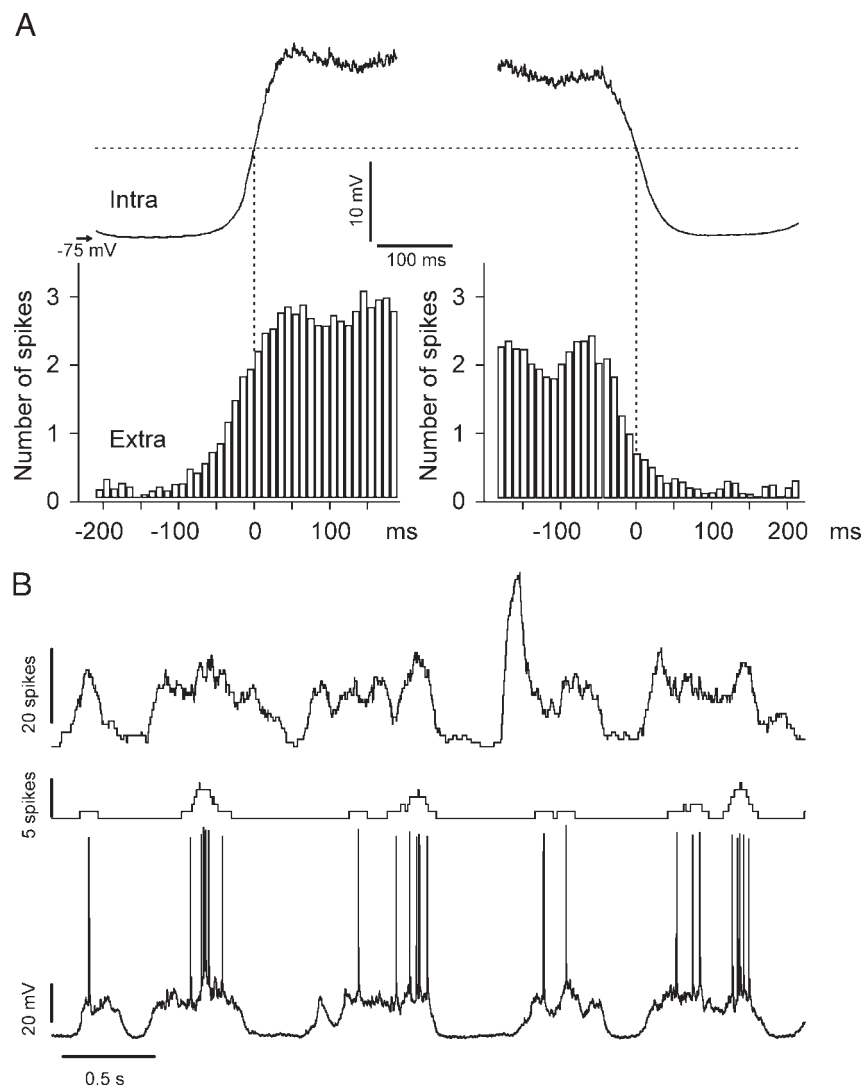


FIG. 7. Level of network activity is higher at a “down”-to-“up” midtransition than at the same membrane potential during an “up”-to-“down” transition. *A*: average membrane potential of an intracellularly recorded neuron during transition from “down”-to-“up” states (*top left*) and from “up”-to-“down” states (*top right*), together with the histograms of simultaneous occurrences of spikes recorded extracellularly from 4 tetrodes in the vicinity (*bottom left and right*, cf. Fig. 1). The presented profiles correspond to averages of 267 (*left*) and 265 (*right*) transitions extracted from a 250-s-long recording. Histogram bars show extracellular average spike counts over 10-ms bins. At the intracellular “down”-to-“up” midtransition (horizontal dashed line), the network activity in the example shown has on average already attained 78.3% of its value at 200 ms after the transition (the “up” state reference value at the time chosen to apply the stimuli in the “up” states in Figs. 2 and 4). By contrast, when the averaged “up”-to-“down” state transition reaches the same membrane potential value, the network activity has already fallen to only 23.3% of the “up” state reference value. Therefore at midway of the “down”-to-“up” and “up”-to-“down” transitions, the intracellularly recorded neuron has on average the same membrane potential but experiences strongly different levels of input activity. *B*: 4 s of simultaneous intra- and extracellular recordings of the group of neurons used to plot the averaged transition profiles shown in *A*. *Bottom*: membrane potential of the intracellularly recorded neuron. *Middle*: trace representing the spike rate of the intracellularly recorded neuron. *Top*: trace representing the overall spike rate of all simultaneously recorded neurons from the 4 tetrodes. Spike rates were computed as described in the legend of Fig. 1.

pyramidal neurons stimulated through their Schaffer collaterals (Pouille and Scanziani 2001).

3) *Synaptic depression*. During the “up” state, the inputs to the recorded neuron are spontaneously active and thus could be affected by synaptic depression, which would cause a decrease in PSP amplitude (Abbott et al. 1997). However, synaptic depression cannot account for the observed reduction in PSP duration.

4) *Refractoriness of stimulated fibers*. Some of the neurons activated by stimulation during the “down” state may participate in the ongoing activity during the “up” state and thus may not be able to respond to the stimulus because of refractoriness. However, considering that frontal cortex neurons have a typical average firing rate between 1 and 10 spikes/s (the firing rate in the “up” state, averaged over all neurons included in this study, was 4.5 spikes/s,  $n = 30$ ), and assuming a refractory period  $\leq 10$  ms for axons, a maximum of only 1 to 10% of the fibers spiking in response to the stimulus in the “down” state would be refractory in the “up” state. Thus refractoriness would only slightly decrease PSP amplitude and would, again, not affect PSP duration.

On the basis of the considerations given above, we propose that the main causes for the observed modulation of PSP shape

reside in the network activity–dependent modulation of the cell’s input resistance and the strong likely contribution of indirectly stimulated inhibition.

#### Linearity of input summation

Studies of synaptic summation performed in various in vitro preparations find both complex nonlinear (Comes et al. 2001; Nettleton and Spain 2000; Schiller et al. 2000; Yoshimura et al. 2000) and linear (Cash and Yuste 1998, 1999) integration. These seemingly contradictory findings may well reflect specific differences between brain areas, for example, cortex (nonlinear) (Nettleton and Spain 2000; Schiller et al. 2000; Yoshimura et al. 2000) versus hippocampus (linear) (Cash and Yuste 1999)—or types of in vitro preparations—acute slice (nonlinear) (Nettleton and Spain 2000; Schiller et al. 2000; Yoshimura et al. 2000) versus cell culture (linear) (Cash and Yuste 1998). They can also reflect specific mechanisms associated with the particular spatial configuration of the stimulations, as was shown with clustered inputs to cortical neurons’ basal dendrites (Schiller et al. 2000). Such site-dependent mechanisms could not be investigated here because our mode of stimulation did not allow for such spatially controlled

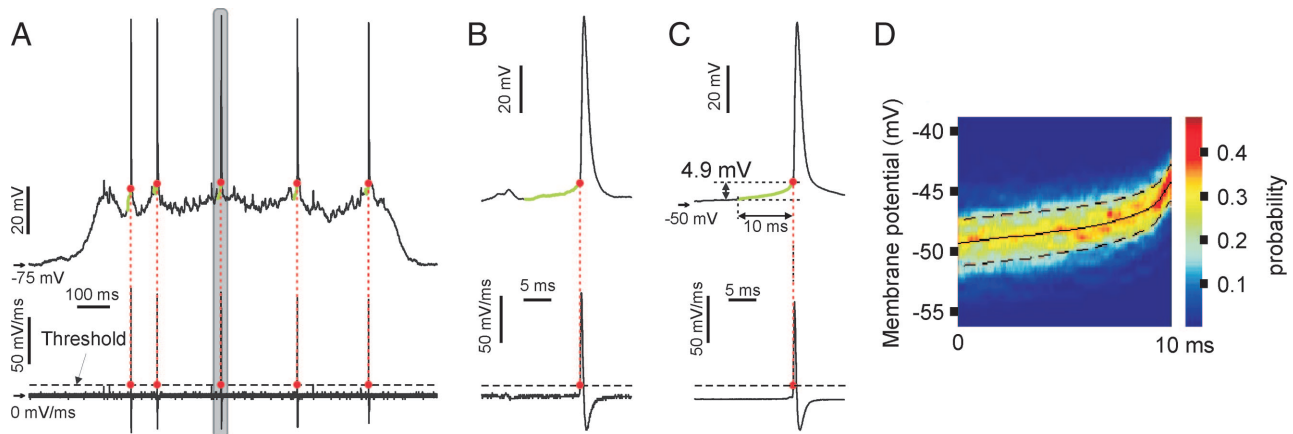


FIG. 8. Time course of depolarization leading to action potentials. *A*: illustration of the method used for calculating action potential threshold. Membrane potential  $V$  (top) and its first-order derivative  $dV/dt$  (bottom) are shown for 1 s of spontaneous activity. Threshold for action potential generation (red dot) was marked every time the derivative of the membrane potential first reached a value higher than the maximum value found during intervals between spikes. Membrane potential during the 10 ms preceding spike onset (i.e., threshold value) is marked in green. *B*: expanded view of the window marked in gray in *A*. *C*: spike-triggered average of membrane potential for all the action potentials recorded during 1 min of spontaneous activity of the neuron presented in Figs. 2 and 4 ( $n = 207$  spikes, firing rate = 3.45 spikes/s). All traces are aligned on spike onset, i.e., threshold crossing (red dot). In the example shown, the membrane potential was on average  $4.9 \pm 1.3$  mV below threshold at 10 ms before spike onset. *D*: probability density (probability per mV as indicated in color scale) of all 207 membrane potential trajectories during 10 ms preceding spike onset for this neuron. Continuous line: average trajectory (cf. Fig. 8C); dashed lines: average  $\pm$  SD of ensemble of trajectories.

activation of synapses. Our results are consistent with other *in vivo* work showing that the summation of visually evoked inputs to neurons in cat visual cortex is linear (Jagadeesh et al. 1993).

#### Synchronization of inputs and spike generation

The strong influence of ongoing network activity on the size and shape of PSPs has a profound influence on the degree of input synchronization needed to elicit postsynaptic spikes. Based on our data we can estimate the precision of input synchronization needed to elicit a response spike. In the presence of ongoing activity (i.e., during the “up” state), the neuron’s integration time window for synaptic input is at most 10 ms, the duration of the average PSP (Fig. 4*B*). Our analysis of the voltage trajectories preceding action potentials revealed that for one PSP duration (i.e., 10 ms) before spike onset the membrane potential was, on average, still almost 5 mV below spike threshold (Fig. 8). Adopting an average amplitude of single cortical EPSPs of 0.1 mV (Matsumura et al. 1996; i.e., 1/5–1/10 of our compound PSPs) and assuming that synaptic transmission failures and amplitude variability of EPSPs are not correlated across input synapses, we would need an excess of  $\geq 60$  unit EPSPs arriving within 10 ms to account for such a sharp increase in prespike membrane potential. Assuming that the neuron receives 10,000 uncorrelated Poisson-distributed excitatory inputs, each firing on average at 4.5 spikes/s (the firing rate in the “up” state, averaged over all neurons included in this study,  $n = 30$ ), the probability of obtaining such an excess number of EPSPs within 10 ms by chance amounts to  $P = 0.003$  at most (see METHODS). It can be shown that this probability is far too small to explain the observed firing rate of the recorded neuron (3.45 spikes/s). Thus we conclude that spiking activity in the cortical network is to a large extent governed by coordinated synchronous presynaptic activity (Abeles 1991; Azouz and Gray 2000; Destexhe and Paré, 1999; Stern et al. 1997).

In a recent modeling study we showed that under physiological conditions, feedforward connected pools of 50–100 neurons can sustain stable transmission of precisely ( $\pm 1$ –3 ms) synchronous spiking activity in a spontaneously active neocortical network (Diesmann et al. 1999). Our experimental findings support these theoretical predictions by showing that the same number of synchronized inputs is both sufficient and necessary to reliably drive single cortical neurons to spike at the observed rate in the presence of ongoing network activity.

#### Modulation of network activity within active epochs

The cortical network is not always in a state of spontaneous, that is, more or less stationary, activity. In fact, considerable modulations in the level of network activity have been observed during task performance (Fetz 1992) and during periods of sustained attention (Steinmetz et al. 2000). According to the mechanism described in our study, we expect such modulations in network activity to cause substantial modulations in input resistance of individual neurons and thus associated modulations in PSP amplitudes and integration time windows. Partial evidence for such effects comes from intracellular recordings in cat visual cortex *in vivo* (Azouz and Gray 1999; Lampl et al. 1999). A comparison between the time courses of depolarization leading to action potential firing during spontaneous activity and during stimulus evoked activity (Azouz and Gray 1999) revealed that the duration of the rising phase before spike onset (the equivalent of the green voltage trajectories in our Fig. 8, *B* and *C*) decreased as the input frequency to the cell increased (cf. Fig. 9 in Azouz and Gray 1999). Thus during periods of evoked activity associated with high levels of background activity, the integration of the depolarizing events triggering spikes was restricted to a shorter time interval. We interpret this result as confirming our finding that increasing network activity shortens the neuronal integration time window. Further evidence comes from the differences in membrane potential fluctuations of simultaneously recorded neurons in primary visual cortex during spontaneous and stimulus-

evoked activity (Lampl et al. 1999). Under spontaneous conditions, the membrane potentials of neurons recorded in close proximity (within 500  $\mu\text{m}$ ) exhibited highly correlated fluctuations, with a broad peak in the center of the cross-correlogram. During visual stimulation, when the neurons received vigorous synaptic inputs, the peak in the correlogram narrowed significantly (see Fig. 8D of Lampl et al. 1999). On the basis of our data, we propose that the narrowing of the correlogram peak reflects the shortening of the postsynaptic potentials (i.e., of the neurons' integration time window) with increased network activity.

In conclusion, the influence of network activity on synaptic integration described in our study has 2 important functional consequences. First, it forces the network to provide its neurons with synaptic inputs that have a degree of synchrony exceeding a minimum "above chance" level. Second, it provides the network with a powerful mechanism to selectively detect and use patterns of synchronously active neurons. By acting as an adaptive filter, with time constants adjusted by the background activity level, it leaves only highly synchronized input patterns effective. Thus our experimental results add to the accumulating evidence that precisely coordinated timing of spikes plays an important role in neocortical processing and computation.

#### ACKNOWLEDGMENTS

We thank M. Abeles, L. Borg-Graham, A. Destexhe, U. Egert, P. Jonas, and S. Rotter for valuable comments on an earlier version of the manuscript, and S. Maier for technical assistance.

#### GRANTS

This work was supported by the Deutsche Forschungsgemeinschaft (SFB505 and Ae10/3), Fondation Fyssen (J.-F. Léger), and the European Commission-Marie Curie program (J.-F. Léger).

#### REFERENCES

- Abbott LF, Varela JA, Sen K, and Nelson SB.** Synaptic depression and cortical gain control. *Science* 275: 220–224, 1997.
- Abeles M.** Role of the cortical neuron: integrator or coincidence detector? *Israel Journal of Medical Sciences* 18: 83–92, 1982.
- Abeles M.** *Corticonics. Neural Circuits of the Cerebral Cortex.* Cambridge, UK: Cambridge Univ. Press, 1991.
- Abeles M, Vaadia E, and Bergman H.** Firing patterns of single units in the prefrontal cortex and neural network models. *Network* 1: 13–25, 1990.
- Amzica F and Steriade M.** Short- and long-range neuronal synchronization of the slow (< 1 Hz) cortical oscillation. *J Neurophysiol* 73: 20–38, 1995.
- Arieli A, Sterkin A, Grinvald A, and Aertsen A.** Dynamics of ongoing activity: explanation of the large variability in evoked cortical responses. *Science* 273: 1868–1871, 1996.
- Azouz R and Gray CM.** Cellular mechanisms contributing to response variability of cortical neurons in vivo. *J Neurosci* 19: 2209–2223, 1999.
- Azouz R and Gray CM.** Dynamic spike threshold reveals a mechanism for synaptic coincidence detection in cortical neurons in vivo. *Proc Natl Acad Sci USA* 97: 8110–8115, 2000.
- Bernander Ó, Douglas RJ, Martin KAC, and Koch C.** Synaptic background activity influences spatiotemporal integration in single pyramidal cells. *Proc Natl Acad Sci USA* 88: 11569–11573, 1991.
- Borg-Graham LJ, Monier C, and Frégnac Y.** Visual input evokes transient and strong shunting inhibition in visual cortical neurons. *Nature* 393: 369–373, 1998.
- Cash S and Yuste R.** Input summation by cultured pyramidal neurons is linear and position-independent. *J Neurosci* 18: 10–15, 1998.
- Cash S and Yuste R.** Linear summation of excitatory inputs by CA1 pyramidal neurons. *Neuron* 22: 383–394, 1999.
- Comes E, Rodriguez V, Léger J-F, Wachtler T, Aertsen A, and Heck D.** Summation of synaptic input in neocortical pyramidal cells in vitro: comparison with in vivo results. *Soc Neurosci Abstr* 31: 501.6, 2001.
- Contreras D and Steriade M.** Cellular basis of EEG slow rhythms: a study of dynamic corticothalamic relationships. *J Neurosci* 15: 604–622, 1995.
- Contreras D, Timofeev I, and Steriade M.** Mechanisms of long-lasting hyperpolarizations underlying slow sleep oscillations in cat corticothalamic networks. *J Physiol* 494: 251–264, 1996.
- Cowan RL and Wilson CJ.** Spontaneous firing patterns and axonal projections of single corticostriatal neurons in the rat medial agranular cortex. *J Neurophysiol* 71: 17–32, 1994.
- Destexhe A and Paré D.** Impact of network activity on the integrative properties of neocortical pyramidal neurons in vivo. *J Neurophysiol* 81: 1531–1547, 1999.
- Diesmann M, Gewaltig MO, and Aertsen A.** Stable propagation of synchronous spiking in cortical neural network. *Nature* 402: 529–533, 1999.
- Fetz EE.** Are movement parameters recognizably coded in the activity of single neurons. *Behav Brain Sci* 15: 679–690, 1992.
- Foehring RC and Surmeier DJ.** Voltage-gated potassium currents in acutely dissociated rat cortical neurons. *J Neurophysiol* 70: 51–63, 1993.
- Heck D, Léger J-F, Stern EA, and Aertsen A.** Size and summation of synchronous and asynchronous population PSPs in rat neo-cortical neurons: intracellular recording in vivo with dual intracortical microstimulation. *Soc Neurosci Abstr* 26: 609.6, 2000.
- Hestrin S.** Different glutamate receptor channels mediate fast excitatory synaptic currents in inhibitory and excitatory cortical neurons. *Neuron* 11: 1083–1091, 1993.
- Jagadeesh B, Wheat HS, and Ferster D.** Linearity of summation of synaptic potentials underlying direction selectivity in simple cells of the cat visual cortex. *Science* 262: 1901–1904, 1993.
- König P, Engel AK, and Singer W.** Integrator or coincidence detector? The role of the cortical neuron revisited. *Trends Neurosci* 19: 130–137, 1996.
- Lampl I, Reichova I, and Ferster D.** Synchronous membrane potential fluctuations in neurons of the cat visual cortex. *Neuron* 22: 361–374, 1999.
- Larkman AU.** Dendritic morphology of pyramidal neurons of the visual cortex of the rat: III. Spine distributions. *J Comp Neurol* 306: 332–343, 1991.
- Magee JC.** Dendritic  $I_h$  normalizes temporal summation in hippocampal CA1 neurons. *Nat Neurosci* 2: 508–514, 1999.
- Magee JC.** Dendritic integration of excitatory synaptic input. *Nat Rev Neurosci* 1: 181–190, 2000.
- Martina M, Schultz JH, Ehmke H, Monyer H, and Jonas P.** Functional and molecular differences between voltage-gated  $K^+$  channels of fast-spiking interneurons and pyramidal neurons of rat hippocampus. *J Neurosci* 18: 8111–8125, 1998.
- Matsumura M, Chen DF, Sawaguchi T, Kubota K, and Fetz E.** Synaptic interactions between primate precentral cortex neurons revealed by spike-triggered averaging of intracellular membrane potential in vivo. *J Neurosci* 16: 7757–7767, 1996.
- Nettleton JS and Spain WJ.** Linear to supralinear summation of AMPA-mediated EPSPs in neocortical pyramidal neurons. *J Neurophysiol* 83: 3310–3322, 2000.
- Nicoll A, Larkman A, and Blakemore C.** Modulation of EPSP shape and efficacy by intrinsic membrane conductances in rat neocortical pyramidal neurons in vitro. *J Physiol* 468: 693–705, 1993.
- Nowak LG and Bullier J.** Axons, but not cell bodies, are activated by electrical stimulation in cortical gray matter. I. Evidence from chronaxie measurements. *Exp Brain Res* 118: 489–500, 1998a.
- Nowak LG and Bullier J.** Axons, but not cell bodies, are activated by electrical stimulation in cortical gray matter. II. Evidence from selective inactivation of cell bodies and axon initial segments. *Exp Brain Res* 118: 489–500, 1998b.
- Paré D, Shink E, Gaudreau H, Destexhe A, and Lang EJ.** Impact of synchronous synaptic activity on the resting properties of cat neocortical pyramidal neurons in vivo. *J Neurophysiol* 79: 1450–1460, 1998.
- Pouille F and Scanziani M.** Enforcement of temporal fidelity in pyramidal cells by somatic feed-forward inhibition. *Science* 293: 1159–1163, 2001.
- Rapp M, Yarom Y, and Segev I.** The impact of parallel fiber background activity on the cable properties of cerebellar Purkinje cells. *Neural Comput* 4: 518–533, 1992.
- Riehle A, Grün S, Diesmann M, and Aertsen A.** Spike synchronization and rate modulation differentially involved in motor cortical function. *Science* 278: 1950–1953, 1997.
- Schiller J, Major G, Koester HJ, and Schiller Y.** NMDA spikes in basal dendrites of cortical pyramidal neurons. *Nature* 404: 285–289, 2000.
- Shu Y, Hasenstaub A, and McCormick DA.** Turning on and off recurrent balanced cortical activity. *Nature* 423: 288–293, 2003.
- Spruston N, Jaffe DB, and Johnston D.** Dendritic attenuation of synaptic

- potentials and currents: the role of passive membrane properties. *Trends Neurosci* 17: 161–166, 1994.
- Steinmetz PN, Roy A, Fitzgerald PJ, Hsiao SS, Johnson KO, and Niebur E.** Attention modulates synchronized neuronal firing in primate somatosensory cortex. *Nature* 404: 187–190, 2000.
- Steriade M, Amzica F, Neckelmann D, and Timofeev I.** Spike-wave complexes and fast components of cortically generated seizures. II. Extra- and intracellular patterns. *J Neurophysiol* 80: 1456–1479, 1998.
- Steriade M, Nuñez A, and Amzica F.** A novel slow (< 1 Hz) oscillation of neocortical neurons in vivo: depolarizing and hyperpolarizing components. *J Neurosci* 13: 3252–3265, 1993.
- Stern EA, Kincaid AE, and Wilson CJ.** Spontaneous subthreshold membrane potential fluctuations and action potential variability of rat corticostriatal and striatal neurons in vivo. *J Neurophysiol* 77: 1697–1715, 1997.
- Tsodyks M, Kenet T, Grinvald A, and Arieli A.** Linking spontaneous activity of single cortical neurons and the underlying functional architecture. *Science* 286: 1943–1946, 1999.
- Yoshimura Y, Sato H, Imamura K, and Watanabe Y.** Properties of horizontal and vertical inputs to pyramidal cells in the superficial layers of the cat visual cortex. *J Neurosci* 20: 1931–1940, 2000.
- Yuste R and Tank DW.** Dendritic integration in mammalian neurons, a century after Cajal. *Neuron* 16: 701–716, 1996.